Combining LoRaWAN and a New 3D Motion Model for Remote UAV Tracking

Federico Mason, Federico Chiariotti, Martina Capuzzo, Davide Magrin, Andrea Zanella, Michele Zorzi
Department of Information Engineering, University of Padova – Via Gradenigo, 6/b, 35131 Padova, Italy
Email: {masonfed, chiariot, capuzzom, magrinda, zanella, zorzi}@dei.unipd.it

Abstract—Over the last few years, the many uses of Unmanned Aerial Vehicles (UAVs) have captured the interest of both the scientific and the industrial communities. A typical scenario consists in the use of UAVs for surveillance or target-search missions over a wide geographical area. In this case, it is fundamental for the command center to accurately estimate and track the trajectories of the UAVs by exploiting their periodic state reports. In this work, we design an ad hoc tracking system that exploits the Long Range Wide Area Network (LoRaWAN) standard for communication and an extended version of the Constant Turn Rate and Acceleration (CTRA) motion model to predict drone movements in a 3D environment. Simulation results on a publicly available dataset show that our system can reliably estimate the position and trajectory of a UAV, significantly outperforming baseline tracking approaches.

I. Introduction

Over the last few years, Unmanned Aerial Vehicles (UAVs) have entered the mainstream: the commercialization of low-cost drones for amateur and professional use is quickly increasing the number of flying units, which will soon be measured in millions, according to the U.S. Federal Aviation Administration (FAA)[1]. Their integration in cellular networks, both as end-users and as coverage extenders [1], is already being discussed, and 5G systems are expected to make use of UAVs of different sizes, from small-scale low-altitude drones to communication satellites [2]. Although energy and battery concerns are still critical [3], the use of UAVs is being proposed for several kinds of scenarios, from remote infrastructure monitoring [4] to disaster monitoring [5] and relief [6].

As the capabilities of UAVs evolve towards the full support of safety-critical applications, accurate positioning of drones is going to become more and more important. Although UAVs often have on-board Global Positioning System (GPS) receivers, filtering [7] and data fusion techniques, often integrating camera image processing [8], can significantly improve the positioning accuracy by combining several measurements into a single solution that is more robust and precise than any individual approach.

In this work, we propose a system to remotely track the position of a UAV moving in a 3D environment. In the considered scenario, a mission control station exploits a novel 3D motion model, called 3-Dimensional CTRA (3D-CTRA), to follow the trajectory of the target. Our model extends the well-known Constant Turn Rate and Acceleration (CTRA) model,

widely used in vehicular scenarios, by adding a third dimension which allows it to represent even complex banking maneuvers accurately. We also study a simpler model, named CTRA+, which considers linear motion on the vertical axis. In both cases, the tracking mechanism is the same: the UAV periodically transmits its state, including the heading, speed and acceleration, and the control station estimates the target position by evolving the motion model. In this way, even sporadic updates allows the system to accurately track the UAV.

In our system, state updates are transmitted through the Long Range Wide Area Network (LoRaWAN) communication standard. This technology allows the transmission of low-bitrate messages at very long distances, enabling the control station to track the drone at ranges of several kilometers with minimal infrastructure. Considering the limited duty cycle imposed by the LoRaWAN specifications, our system can support swarms of up to 72 drones with a packet collision rate below 10% by using different Spreading Factors (SFs) [9]. When LoRaWAN is tuned to achieve larger communication range, the intervals between transmissions can last several seconds, thus making the tracking more difficult. It is hence interesting to analyze the feasibility of such a framework, and to investigate its performance when varying the considered mobility model. We tested our system in extensive ns-3 simulations using the UAV mobility traces from the Mid-Air public dataset and comparing the two mobility models we proposed against a baseline solution implementing Dead Reckoning (DR), a well-known tracking method exploiting a uniform rectilinear motion model to predict the target movements. The results show that the more accurate 3D-CTRA mobility model can bring an improvement of up to 30% on the 75th percentile tracking error.

The rest of the paper is organized as follows. Sec. II presents the state of the art on UAV applications and tracking models, including both GPS and visual data. Sec. III presents the CTRA+ and 3D-CTRA models, including the relative update equations, and describes the LoRaWAN standard and the frequency plan needed for our application. The simulation settings and the results are described in Sec. IV, while Sec. V presents our concluding remarks and ideas for future work.

II. Related work

UAVs' popularity has grown exponentially over the past few years, and their widespread use could enable a real Internet of Flying Robots [10] in the near future. Drones are used

---

[1]FAA Aerospace Forecast, Fiscal Years 2019-2039: https://www.faa.gov/news/updates/?newsId=93646

for environmental monitoring in a wide range of scenarios, from traffic jam detection [11] to industry and agriculture [12], and are posed to become a key Smart City infrastructure [13]. UAVs are also being used in combination with ground-based robots to help them perform complex tasks [14]. However, disaster management and relief is perhaps the most interesting application for UAVs: drones can easily avoid ground-level obstacles and flooded areas by flying over them, surveying the extent of the damage [5] or helping with search and rescue operations [6] and communications. In order to enable these critical services, controllers must be able to follow and even anticipate the drone's trajectory. This requires the UAV to transmit frequent positioning updates [15], often at long ranges.

The target tracking problem is a well-studied research topic, and is usually solved by representing the target's motion using simple models and estimating its position with a Bayesian Filtering (BF) algorithm. The best-known BF algorithms used in this context are the Kalman Filter (KF) [16] and the Particle Filter (PF) [17]. Long-term forecasting can be achieved by simply applying the predictive step of the BF to the last available state estimation. However, this solution does not provide good performance when updates are infrequent, especially if the model is inaccurate. In this perspective, our work tries to minimize broadcasting operations while ensuring accurate position estimation.

The tracking problem has been widely explored in 2D vehicular scenarios [18], often using the CTRA model [19], which considers an accelerating vehicle with constant turn rate. A similar model for drones moving horizontally was presented in [20], including Gaussian noise on the motion parameters. A more complex model with several possible maneuvers was described in [21], adapting the CTRA settings to draw the correct trajectory. In general, motion models for drones are based on 2D CTRA or simpler models with constant speed [22] or heading [23]. To the best of our knowledge, our CTRA+ and 3D-CTRA models are the first models that can represent 3D maneuvers with the same flexibility that CTRA has in the 2D space.

III. SYSTEM MODEL

In this work, we model a UAV which periodically transmits its state to a control station using the LoRaWAN communication standard. The aim of the control station is to accurately track the UAV position in different scenarios. To represent the drone motion in a 3D environment, we consider three possible models, i.e., DR, CTRA+, and 3D-CTRA. In the rest of the section, we first extend conventional CTRA, obtaining the system equations for CTRA+ and 3D-CTRA. Then, we analyze the tracking and communication frameworks.

A. The CTRA+ model

While standard CTRA only tracks the yaw, i.e., the angle θ between the drone's heading and the reference direction on the horizontal plane, 3D motion models must also consider the pitch, i.e., the vertical angle ϕ between the drone's heading and the horizon. Moreover, the target state must include the

altitude z as well as the horizontal position (x, y), resulting in the 5-tuple (x, y, z, θ, ϕ). These parameters are common to all the motion models we implement. However, none of our models explicitly considers roll, which is not strictly necessary to represent motion in a 3D space.

In 2D CTRA, the turn rate $\omega = \frac{d\theta}{dt}$ is assumed to be constant. The CTRA+ model makes the same assumption and, moreover, considers a constant pitch ϕ:

$$\theta(t) = \theta(0) + \omega t \quad (1)$$

$$\phi(t) = \phi(0), \quad (2)$$

where $\theta(0)$ and $\phi(0)$ represent the initial heading of the drone.

Like standard CTRA, CTRA+ assumes the tangential acceleration $a = \frac{dv}{dt}$ to be constant, which turns the circular motions into Archimedean spirals [24]. In particular, CTRA+ considers the spirals on a plane tilted by an angle ϕ with respect to the horizon. By projecting the UAV's velocity vector $\mathbf{v}(t)$, we can get its three components:

$$v_x(t) = \frac{dx}{dt} = v(t)\cos(\theta(t))\cos(\phi(t)); \quad (3)$$

$$v_y(t) = \frac{dy}{dt} = v(t)\sin(\theta(t))\cos(\phi(t)); \quad (4)$$

$$v_z(t) = \frac{dz}{dt} = v(t)\sin(\phi(t)). \quad (5)$$

Therefore, the velocity's magnitude $v(t)$ is given by:

$$v(t) = (v_x(t))^2 + (v_y(t))^2 + (v_z(t))^2. \quad (6)$$

In order to compute the position at any time, we need to integrate the velocity components over time:

$$x(t) = x(0) + \int_0^t v(\tau)\cos(\theta(\tau))\cos(\phi)d\tau; \quad (7)$$

$$y(t) = y(0) + \int_0^t v(\tau)\sin(\theta(\tau))\cos(\phi)d\tau; \quad (8)$$

$$z(t) = z(0) + \int_0^t v(\tau)\sin(\phi)d\tau. \quad (9)$$

We note that the procedure is equivalent to 2D CTRA [19] for the x and y components, except for the constant multiplying factor $\sin(\phi)$. Hence, the CTRA+ state is given by:

$$\mathbf{x}_{\text{CTRA+}}(t) = [x(t)\ y(t)\ z(t)\ \theta(t)\ \phi\ v(t)\ a\ \omega]^T, \quad (10)$$

which corresponds to the tuple representing the current attitude, with the addition of the velocity v, the acceleration a, and the turn rate ω.

B. The 3D-CTRA model

The 3D-CTRA model extends the above description by adding a constant tilt rate $\psi = \frac{d\phi}{dt}$. Consequently, the UAV's movement is represented as the combination of two independent spiraling motions on the horizontal and vertical planes, forming a curved helix. While the evolution of $\theta(t)$ still follows (1), the pitch is given by:

$$\phi(t) = \phi(0) + \psi t. \quad (11)$$

This complicates the derivation of the motion equations considerably, since $\phi(t)$ is now time-dependent. For the sake of simplicity, we report the procedure only for $x(t)$, which is given by

$$x(t) = x(0) + \int_0^t v(\tau)\cos(\theta(\tau))\cos(\phi(\tau))d\tau. \quad (12)$$

Applying the Werner formula, we obtain

$$x(t) = x(0) + \int_0^t \frac{v}{2}\big(\cos(\theta(\tau) + \phi(\tau)) \\ + \cos(\theta(\tau) - \phi(\tau))\big)d\tau, \quad (13)$$

which can be solved in closed form. The derivations for $y(t)$ and $z(t)$ follow the same steps: the final results are given in (14)-(16), on top of next page, where we used the compact notation $[F(x)]_a^b = F(b) - F(a)$ to indicate that the primitive function $F(x)$ should be evaluated at the extremes a and b.

Finally, three special cases need to be considered. First, when $\psi = 0$, i.e., when the model is equivalent to CTRA+ and the pitch is constant, the value of $z(t)$ becomes:

$$z(t) = z(0) + \sin(\phi(t))\left(v(t)t - \frac{at^2}{2}\right). \quad (17)$$

Then, when $\omega = \psi$, i.e., the rotations on the two axes have the same period, the values of $x(t)$ and $y(t)$ become:

$$x(t) = \left[\frac{v(\tau)\sin(\theta(\tau) + \phi(\tau))}{2(\omega + \psi)} + \frac{a\cos(\theta(\tau) + \phi(\tau))}{2(\omega + \psi)^2} + \left(\frac{v(\tau)\tau}{2} - \frac{a\tau^2}{4}\right)\cos(\theta(\tau) - \phi(\tau))\right]_0^t + x(0) \quad (18)$$

$$y(t) = \left[-\frac{v(\tau)\cos(\theta(\tau) + \phi(\tau))}{2(\omega + \psi)} + \frac{a\sin(\theta(\tau) + \phi(\tau))}{2(\omega + \psi)^2} + \left(\frac{v(\tau)\tau}{2} - \frac{a\tau^2}{4}\right)\sin(\theta(\tau) - \phi(\tau))\right]_0^t + y(0) \quad (19)$$

The case in which $\omega = -\psi$ produces a similar result, with inverted terms. Setting $t = T$, (1), (11) and (14)-(16), or their special case equivalents, define the full non-linear version of the 3D-CTRA model with step T. In particular, the 3D-CTRA state is given by:

$$\mathbf{x}_{\text{3D-CTRA}}(t) = [x(t)\ y(t)\ z(t)\ \theta(t)\ \phi(t)\ v(t)\ a\ \omega\ \psi]^T, \quad (20)$$

which is equivalent to (10), with the addition of the tilt rate ψ.

We observe that 3D-CTRA considers constant values for both ω and ψ. This does not reflect the real behavior of an aircraft, as dives and climbs are usually relatively short. To overcome this problem and make the model more realistic, we make the tracking system reduce the value of ψ by a factor η after every prediction step. In other words, the model assumes that the drone will gradually reduce its tilt rate and stabilize its pitch.

C. Remote tracking and communications

As in [19], the tracking process is implemented by the Unscented Kalman Filter (UKF) algorithm. In particular, we assume that the UAV and the control station are equipped with two UKFs [25]. While the drone exploits the measurements provided by its on-board sensors to track its own state, the control station's UKF has no input but the information received from the UAV. We adopt a periodic broadcasting strategy [18]: the UAV sends the estimate of its own state to the control station with a constant inter-transmission period. After it receives an update, the control station updates its UKF with the new information and exploits the predictive step to forecast the UAV's trajectory. Naturally, the errors will compound, causing long-term predictions to become less and less accurate until the next update.

In order to enable the UAV to send the UKF parameters even at great distances, we considered the LoRaWAN technology [26], which leverages the proprietary LoRa PHY modulation which is based on a chirp spread spectrum technique to transmit over long distances. The performance of the modulation can be tuned through the SF parameter, which takes values from 7 to 12, and allows to trade coverage range for data rate: signals transmitted with higher SFs values require longer transmission times, but are more robust to channel impairments and, thus, can be received at farther distances, up to several kilometers in open-air scenarios.

LoRaWAN is based on a star topology, with three kinds of devices:

- the *Network Server (NS)*, which is the central network controller;
- the *End Devices (EDs)*, peripheral nodes, collecting data and transmitting them through the LoRa modulation;
- the *Gateways (GWs)*, acting as relays between EDs and NS, collecting messages from devices and forwarding them to the controller through a legacy IP connection, and *vice-versa*.

We assume that the drone is equipped with a LoRaWAN *Class A* ED. This class is designed to consume a minimum amount of energy, staying in sleep mode most of the time, transmitting when necessary, and opening two short windows for reception after each transmission. LoRaWAN works in the unlicensed 868 MHz sub-band, which is subject to Duty Cycle (DC) regulations. In particular, three 125 MHz channels are allocated to Uplink (UL) transmissions, and must respect a DC limitation of 1%. Another option is to use a single 250 MHz channel, which does not bring the benefits of frequency orthogonality but reduces the packet transmission time, and is preferable in case of a system with a single drone.

Because of the DC limitation, we need to compress the system state to reduce the inter-transmission time and improve the tracking performance. In order to minimize the payload size, we can represent the position using 2 bytes, allowing movement in a square box with a size of 13 km while limiting the quantization error to 10 cm, significantly less than the average GPS error. Angles and turn rates can be represented using just 1 byte, with a maximum error of 0.7 degrees;

$$x(t) = x(0) + \left[\frac{v(\tau)\sin(\theta(\tau) + \phi(\tau))}{2(\omega + \psi)} + \frac{v(\tau)\sin(\theta(\tau) - \phi(\tau))}{2(\omega - \psi)} + \frac{a\cos(\theta(\tau) + \phi(\tau))}{2(\omega + \psi)^2} + \frac{a\cos(\theta(\tau) - \phi(\tau))}{2(\omega - \psi)^2} \right]_0^t \tag{14}$$

$$y(t) = y(0) + \left[-\frac{v(\tau)\cos(\theta(\tau) + \phi(\tau))}{2(\omega + \psi)} - \frac{v(\tau)\cos(\theta(\tau) - \phi(\tau))}{2(\omega - \psi)} + \frac{a\sin(\theta(\tau) + \phi(\tau))}{2(\omega + \psi)^2} + \frac{a\sin(\theta(\tau) - \phi(\tau))}{2(\omega - \psi)^2} \right]_0^t \tag{15}$$

$$z(t) = z(0) + \left[-v(\tau)\frac{\cos(\phi(\tau))}{\psi} + a\frac{\sin(\phi(\tau))}{\psi^2} \right]_0^t. \tag{16}$$
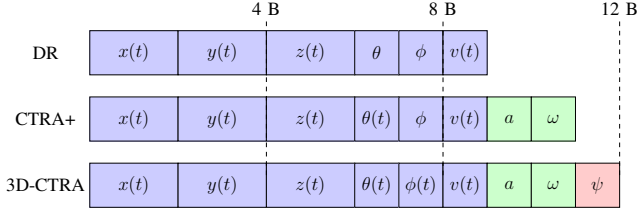

Figure 1: Schematic of the payload format for the three tracking schemes

since velocity and acceleration are limited, they can also be represented with just 1 byte, with a negligible loss of precision. Since DR tracking requires the knowledge of the attitude 5-tuple and the velocity, its minimum payload size is 9 bytes. The CTRA+ state as given in (10) requires 11 bytes, and the 3D-CTRA state as given in (20) requires 12 bytes. The different payload formats are reported in Fig. 1. The LoRa transmission times for packets with these lengths are reported in Tab. I: to respect the DC limitation, packets can be sent only sporadically, with a transmission period in the order of a few seconds.

IV. SIMULATION SETTINGS AND RESULTS

To simulate the scenario described in the previous section, we exploit the Mid-Air dataset [27], which contains the flying records of a quad-copter moving in 3 different virtual environments. In particular, we consider 30 trajectories for a total flying duration of 44 minutes. These data are used to represent the ground-truth motion of the target while we synthetically generated noisy data to represent the information acquired with the drone's sensors. The sensor data included the position, the attitude, and the velocity and acceleration vectors of the UAV, combining GPS, accelerometer and gyroscope. In the rest of the section, we describe the setting of our simulations and we present the obtained results.

A. Settings

In our scenario, the control station is located at a distance d from the drone. The process noise of the tracking system

is described by the matrix $Q = qI$, where I represents the identity matrix. Instead, the error affecting the drone measurements is given by a diagonal matrix R, whose elements represent the accuracy of the various drone sensors. The noise matrices and the UKF parameters are reported in Tab. II. In particular, values of R were chosen according to [28]–[30]. We highlight that the UKF setting, e.g., the state dimension, changes according to the chosen motion model. As already stated, the UKF at the control station is used to estimate the target trajectory by exploiting only the predictive step. This implies that, when a new update is received, the filter state is substituted with the new information, and the estimation process starts again.

The scenario of interest was studied with the network simulator ns-3, with a single drone moving in the space according to the mobility traces of [31]. The drone was equipped with a LoRaWAN interface, which transmitted packets at the maximum frequency allowed by the DC. These messages were collected by a GW, and forwarded to a NS. Transmitted packets did not require any acknowledgment, and the NS did not control any of the communication parameters. For each packet, we recorded whether it was successfully received or not, and estimate the tracking performance. We also moved the initial position of the GW to see how much the tracking performance was affected by the communication limitations. In the rest of the section, we will analyze the positioning error for different tracking and communication scenarios. In particular, we investigate our tracking scheme for different values of the SF and of the initial distance d between the UAV and the GW.

B. Results

First, we consider the 30 s drone trajectory shown in Fig. 2. The same figure includes the trajectories estimated by the control station using the DR and 3D-CTRA motion models, considering a communication setup with $d = 1000$ m, SF = 7 and $B = 250$ MHz. Comparing the different trajectories,

SF	B (MHz)	Packet size (B)	Transmission time (s)	Min transmission interval (s)
7	125	9, 11, 12	0.0412	4.21
	250	9, 11, 12	0.0206	2.06
8	125	9	0.0722	7.22
		11, 12	0.0824	8.24
	250	9	0.0391	3.61
		11, 12	0.0412	4.12

Table I: Transmission times for packets with the three different payloads and minimum transmission interval required to respect DC regulations with the standard frequency plan.

| Parameter	Value	Description
R_x	$0.8274\ m^2$	Position accuracy along x
R_y	$0.8274\ m^2$	Position accuracy along y
R_z	$3.7481\ m^2$	Position accuracy along z
R_v	$0.2500\ (m/s)^2$	Speed accuracy
R_a	$0.1521\ (m/s^2)^2$	Acceleration accuracy
R_θ	$0.0085\ rad^2$	Yaw accuracy
R_ϕ	$0.0085\ rad^2$	Pitch accuracy
R_ω	$0.0003\ (rad/s)^2$	Turn rate accuracy
R_ψ	$0.0003\ (rad/s)^2$	Tilt rate accuracy
q	0.1	Process noise matrix parameter
η	0.9	Tilt reduction parameter

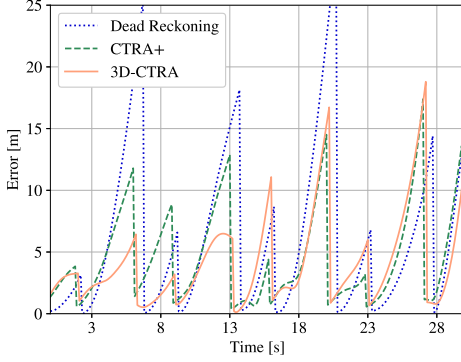Table II: Tracking system parameters.
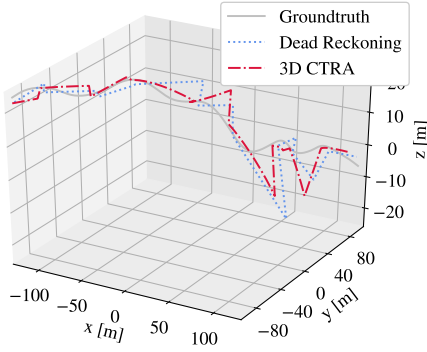
Figure 2: 3D trajectory of the UAV.

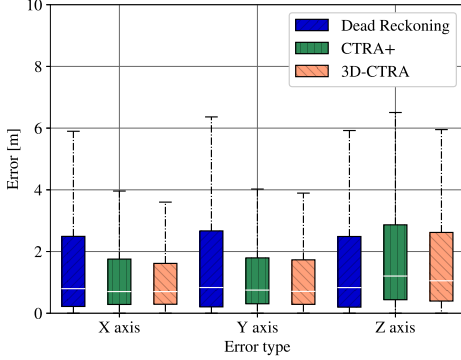Figure 3: Error over time with $d = 1000$ m, SF = 7 and $B = 250$ MHz.

Figure 4: Error over the three axes with $d = 1000$ m with SF = 7 and $B = 250$ MHz.

Figure 5: Error for different values of d with SF = 7 and $B = 250$ MHz.
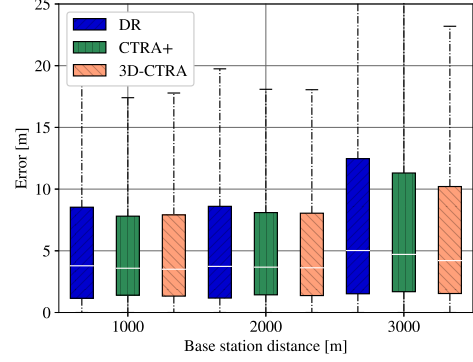
Figure 6: Error for different values of d with SF 8 and $B = 250$ MHz.

we observe how the DR scheme does not follow the target while the 3D-CTRA scheme has smaller deviations from the real trajectories. This is confirmed by the results in Fig. 3, which shows the base station tracking error over time for all the considered models. We highlight that the error of the DR model rapidly increases every time the drone performs non-linear movements, as it happens at time $t \simeq 6, 12, 19$ s. Instead, the error of both the CTRA+ and the 3D-CTRA models presents a smoother trend, with fewer and lower peaks.

From here on, we consider the cumulative results over all the available trajectories. Fig. 4 shows the boxplot of the position error along the three axes with SF = 7, $d = 1000$ m, and $B = 250$ MHz. We observe that, when considering the X and Y axes, the 3D-CTRA model always outperforms both the DR and the CTRA+ models, thanks to its richer representation of the drone's movements. As expected, CTRA+ also
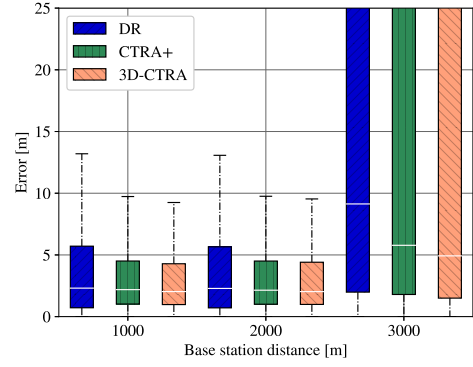
outperforms DR, since it uses the same model as 3D-CTRA on the horizontal plane. Surprisingly, when considering the Z axis, the DR system shows a slightly lower error than CTRA+ and 3D-CTRA. This might be due to climbs and dives being relatively rare, so DR's more frequent updates could give it a slight edge over 3D-CTRA. On this axis, CTRA+ performs worst, because it combines the lower update frequency of 3D-CTRA and the inaccurate model of DR.

We now evaluate how the communication parameters can affect the performance of the tracking system. Fig. 5 shows the boxplot of the positioning error for different values of d and considering SF = 7 and $B = 250$ MHz. It is easy to see that 3D-CTRA outperforms the other approaches, even if its updates are less frequent. In particular, considering $d = 1000$ m, the 75th percentile of the error obtained with the 3D-CTRA model is 30% lower than DR's and 10% lower than CTRA+'s. We observe that all the systems guarantee an average error below 2 m for both $d = 1000$ m and $d = 2000$ m. However, the error dramatically increases when considering $d = 3000$ m for all the considered schemes, since the drone is too far away from the control station for SF = 7 and several packets are lost. However, 3D-CTRA is still the best option: it is the only one to guarantee an average error below 5 m.

To allow the control station to accurately predict the drone's trajectory at larger distances, it is necessary to adopt a more robust communication setting. In Fig. 6, we report the results we obtained for $d \in \{1000, 2000, 3000\}$, with SF = 8 and $B = 250$ MHz. Since we increased the SF, the bitrate is lower, and the drone transmits its state less frequently. As expected, this implies that the positioning error increases at short distances.

For $d = 1000$ m and $d = 2000$ m, the 3D-CTRA model guarantees lower error than the DR model but presents similar results to the CTRA+ model. Instead, in the case of $d = 3000$ m, 3D-CTRA outperforms both the other techniques: the 75th percentile error obtained with the 3D-CTRA is 20% lower than DR's and 12.5% lower than CTRA+'s.

Finally, comparing Fig. 5 and Fig. 6 shows how a more robust scheme greatly improves the tracking performance when the distance between the control station and the UAV is large. It is worth noting that LoRaWAN also provides a Data Rate Adaptation mechanism, where the SF employed by the device is set by the controller: in this way, it is possible to benefit from the increased coverage range achieved with higher SF when necessary, and go back to lower SFs when the UAV is closer to the GW to increase the frequency of transmission messages. Therefore, adapting the SF dynamically will be the best choice in a real scenario, providing significant performance gains. However, the reactiveness of the adaptive mechanism should be carefully tuned to avoid instability.

V. Conclusions and future work

In this work, we presented a tracking system for UAVs, based on a novel 3D-CTRA mobility model and on periodic transmissions over LoRaWAN. Our system can track a drone's trajectory with high accuracy even when the drone is at 3 km from the LoRaWAN gateway, and the mobility models we propose significantly outperform standard DR. Moreover, LoRaWAN's duty cycle limit is suited to manage swarms of dozens of drones, as it prevents traffic congestion.

There are several possible avenues of future work: a refinement of the movement model, including maneuver and mission-level information, might reduce the tracking error. From the communication side, it would be interesting to investigate the tracking performance with different data rate adaptation algorithms, as well as explore features that are not part of the LoRaWAN standard up to now, like the use of a different frequency plan or of listen-before-talk instead of applying the duty cycle. Finally, the study of the behavior of swarms, and possible strategies to avoid packet collision, is another interesting option that would enable new applications by improving the tracking accuracy at low cost.

References

[1] A. Fotouhi, H. Qiang, M. Ding, M. Hassan, L. G. Giordano, A. Garcia-Rodriguez, and J. Yuan, "Survey on UAV cellular communications: Practical aspects, standardization advancements, regulation, and security challenges," *IEEE Communications Surveys & Tutorials*, Mar. 2019.

[2] S. Sekander, H. Tabassum, and E. Hossain, "Multi-tier drone architecture for 5G/B5G cellular networks: Challenges, trends, and prospects," *IEEE Communications Magazine*, vol. 56, no. 3, pp. 96–103, Mar. 2018.

[3] T. Long, M. Ozger, O. Cetinkaya, and O. B. Akan, "Energy neutral Internet of Drones," *IEEE Communications Magazine*, vol. 56, no. 1, pp. 22–28, Jan. 2018.

[4] B. Hament and P. Oh, "Unmanned aerial and ground vehicle (UAV-UGV) system prototype for civil infrastructure missions," in *IEEE International Conference on Consumer Electronics (ICCE)*. IEEE, Jan. 2018, pp. 1–4.

[5] S. Zakaria, M. R. Mahadi, A. F. Abdullah, and K. Abdan, "Aerial platform reliability for flood monitoring under various weather conditions: A review," in *GeoInformation for Disaster Management Conference*. Springer, Mar. 2018, pp. 295–314.

[6] J. Scherer, S. Yahyanejad, S. Hayat, E. Yanmaz, T. Andre, A. Khan, V. Vukadinovic, C. Bettstetter, H. Hellwagner, and B. Rinner, "An autonomous multi-UAV system for search and rescue," in *Proceedings of the First Workshop on Micro Aerial Vehicle Networks, Systems, and Applications for Civilian Use*. ACM, May 2015, pp. 33–38.

[7] J. Dentler, S. Kannan, M. A. O. Mendez, and H. Voos, "A real-time model predictive position control with collision avoidance for commercial low-cost quadrotors," in *IEEE Conference on Control Applications (CCA)*. IEEE, Sep. 2016, pp. 519–525.

[8] C. V. Angelino, V. R. Baraniello, and L. Cicala, "UAV position and attitude estimation using IMU, GNSS and camera," in *15th International Conference on Information Fusion*. IEEE, Jul. 2012, pp. 735–742.

[9] J. Haxhibeqiri, F. Van den Abeele, I. Moerman, and J. Hoebeke, "Lora scalability: A simulation model based on interference measurements," *Sensors*, vol. 17, no. 6, p. 1193, May 2017.

[10] H. Huang and A. V. Savkin, "Towards the Internet of Flying Robots: A survey," *Sensors*, vol. 18, no. 11, p. 4038, Nov. 2018.

[11] V. Sharma, I. You, G. Pau, M. Collotta, J. Lim, and J. Kim, "LoRaWAN-based energy-efficient surveillance by drones for intelligent transportation systems," *Energies*, vol. 11, no. 3, p. 573, Mar. 2018.

[12] D. Vasisht, Z. Kapetanovic, J. Won, X. Jin, R. Chandra, S. Sinha, A. Kapoor, M. Sudarshan, and S. Stratman, "Farmbeats: An IoT platform for data-driven agriculture," in *14th Symposium on Networked Systems Design and Implementation (NSDI)*. USENIX, Sep. 2017, pp. 515–529.

[13] A. Ismail, B. Bagula, and E. Tuyishimire, "Internet-of-things in motion: A UAV coalition model for remote sensing in smart cities," *Sensors*, vol. 18, no. 7, p. 2184, Jul. 2018.

[14] B. Arbanas, A. Ivanovic, M. Car, M. Orsag, T. Petrovic, and S. Bogdan, "Decentralized planning and control for UAV–UGV cooperative teams," *Autonomous Robots*, vol. 42, no. 8, pp. 1601–1618, Dec. 2018.

[15] I. Jawhar, N. Mohamed, J. Al-Jaroodi, D. P. Agrawal, and S. Zhang, "Communication and networking of UAV-based systems: Classification and associated architectures," *Journal of Network and Computer Applications*, vol. 84, pp. 93–108, Apr. 2017.

[16] R. Kalman, "A new approach to linear filtering and prediction problems," *Transactions of the ASME - Journal of basic Engineering*, vol. 82, pp. 35–45, 01 1960.

[17] P. Del Moral, "Non-linear filtering: interacting particle resolution," *Markov processes and related fields*, vol. 2, no. 4, pp. 555–581, 1996.

[18] F. Mason, M. Giordani, F. Chiariotti, A. Zanella, and M. Zorzi, "Quality-aware broadcasting strategies for position estimation in VANETs," in *European Wireless Conference (EW)*. IEEE, May 2019.

[19] M. Tsogas, A. Polychronopoulos, and A. Amditis, "Unscented Kalman filter design for curvilinear motion models suitable for automotive safety applications," in *7th International Conference on Information Fusion*, July 2005.

[20] J.-D. M. M. Biomo, T. Kunz, and M. St-Hilaire, "An enhanced Gauss-Markov mobility model for simulations of unmanned aerial ad hoc networks," in *7th IFIP Wireless and Mobile Networking Conference (WMNC)*. IEEE, May 2014, pp. 1–8.

[21] O. Bouachir, A. Abrassart, F. Garcia, and N. Larrieu, "A mobility model for UAV ad hoc network," in *International Conference on Unmanned Aircraft Systems (ICUAS)*. IEEE, 2014, pp. 383–388.

[22] Y. Wan, K. Namuduri, Y. Zhou, and S. Fu, "A smooth-turn mobility model for airborne networks," *IEEE Transactions on Vehicular Technology*, vol. 62, no. 7, pp. 3359–3370, Mar. 2013.

[23] J. Tiemann, F. Schweikowski, and C. Wietfeld, "Design of an UWB indoor-positioning system for UAV navigation in GNSS-denied environments," in *International Conference on Indoor Positioning and Indoor Navigation (IPIN)*. IEEE, Oct. 2015, pp. 1–7.

[24] Archimedes of Syracuse, "Περὶ ἑλίκων (on spirals)," ~225BC.

[25] R. Van Der Merwe *et al.*, "Sigma-point Kalman filters for probabilistic inference in dynamic state-space models," Ph.D. dissertation, OGI School of Science & Engineering at OHSU, 2004.

[26] LoRa Alliance, "LoRaWAN™ 1.1 Specification," Oct. 2017.

[27] M. Fonder and M. V. Droogenbroeck, "Mid-air: A multi-modal dataset for extremely low altitude drone flights," in *Conference on Computer Vision and Pattern Recognition Workshop (CVPRW)*, June 2019.

[28] G. P. Team, "Global Positioning System (GPS) standard positioning service (sps) performance analysis report," 2014.

[29] B. Kim and K. Yi, "Probabilistic and holistic prediction of vehicle states using sensor fusion for application to integrated vehicle safety systems," *IEEE Transactions on Intelligent Transportation Systems*, vol. 15, no. 5, pp. 2178–2190, 2014.

[30] G. Falco, M. Pini, and G. Marucco, "Loose and tight GNSS/INS integrations: Comparison of performance assessed in real urban scenarios," *Sensors*, vol. 17, no. 2, p. 255, 2017.

[31] A. L. Majdik, C. Till, and D. Scaramuzza, "The Zurich urban micro aerial vehicle dataset," *The International Journal of Robotics Research*, vol. 36, no. 3, pp. 269–273, Mar. 2017.